

Electromagnetic Response Studies of the Antenna for Deep Water Deep Target CSEM Environments

Noorhana Yahya¹, Nadeem Nasir^{2,3}, Majid Niaz Akhtar^{2,4}, Muhammad Kashif², Tanvir Hussain⁵,
Hasnah Mohd Zaid¹, Afza Shafie¹

¹Fundamental and Applied Science Department, Tronoh, Malaysia; ²Electrical and Electronic Engineering Department, Tronoh, Malaysia; ³Fundamental and Applied Science Department, National Textile University, Faisalabad, Pakistan; ⁴Comsats Institute of Information Technology Lahore, Lahore, Pakistan; ⁵Mechanical Engineering Department, Universiti Teknologi PETRONAS, Tronoh, Malaysia.
Email: noorhana_yahya@petronas.com.my, nadeemnasirmtu@gmail.com, kashifmughal79@gmail.com, majidniazakhtar@gmail.com

Received September 2nd, 2012; revised October 5th, 2012; accepted October 15th, 2012

ABSTRACT

The Controlled Source Electromagnetic Method (CSEM) is used for offshore hydrocarbon exploration. Hydrocarbon detection in seabed logging (SBL) is a very challenging task for deep hydrocarbon reservoirs. The electromagnetic field response of an antenna is unable to detect deep hydrocarbon reservoirs due to a weak electromagnetic signal response in the seabed logging environment. This work premise deals with the comparison of the electromagnetic signal strength of a new antenna with a straight antenna and the orientation of an antenna for deep target hydrocarbon exploration. Antenna position and orientation (T_x and T_y) was studied using Computer Simulation Technology software (CST) for deep targets in marine CSEM environments. The model area was assigned as (40 × 40 km) to replicate the real seabed environment. From the results, the new dipole antenna shows an 804% and 278% increase in electric and magnetic field strength than the straight antenna. An electric (E) and magnetic (H) field component study was done with and without the presence of a hydrocarbon reservoir. E_x and H_z field component responses with the new antenna at the 1 km target were measured in a deep water environment. It was analyzed that the antenna shows 53.10% (E_x) and 83.13% (H_z) field difference in deep water with and without a hydrocarbon reservoir at the 30 m antenna position from the sea floor. From the antenna orientation results, it was observed that, the electric field E_x and magnetic field H_z responses decreased from 18% to 12% and 21% to 16%, respectively but was still able to detect the deep target hydrocarbon reservoir at the 4 km target depth. This EM antenna may open new frontiers for the oil and gas industry for deep target hydrocarbon detection (HC).

Keywords: Control Source Electromagnetic (CSEM); Seabed Logging (SBL); Antenna; Computer Simulation Technology (CST); Hydrocarbon (HC)

1. Introduction

Seabed logging is an application of the control source electromagnetic method which is used to locate an oil reservoir beneath the sea floor by measuring electromagnetic fields [1-4]. Typically, in the control source method, a horizontal electric dipole antenna is towed by a surface vessel at a short distance from the sea floor [5-7]. The dipole antenna transmits very low frequency electromagnetic waves with frequencies ranging from 0.25 Hz - 10 Hz; due to the low frequency, transmitted energy propagates down through the subsurface [8-10]. Low frequency electromagnetic waves attenuate more in the conductive layer and less in the resistance layer due to the skin depth. In a large resistive layer such as hydrocarbon, electromagnetic energy flows along the re-

servoir (described as a guided wave) and is detected by the stationary sea floor electric or magnetic field detectors which are deployed on the sea floor. The control source electromagnetic method depends on the resistivity of the hydrocarbon and the surrounding sediments. Hydrocarbon in the seabed has resistivity of a few tens to hundred ohm meter (30 Ω m - 500 Ω m), sea water (0.5 Ω m - 2 Ω m) while all other layers including sediments in the sea have resistivity of (1 Ω m - 2 Ω m) [11-18]. A 1D numerical model for a marine CSEM environment with the change of water depth and change of frequency was reported [19]. His proposed model consists of a 1 km-deep target depth, with a sea water layer of (0.3 Ω m) over a (1 Ω m) half-space. A 100 m thick, 100-Ohm-m resistive layer representing a hydrocarbon reservoir is embedded at 1km below the seafloor for the 1D reservoir

proposed model. The antenna length of 250 m is excited with a 200 ampere current with a sinusoidal waveform at different frequencies. An HED Antenna is placed in x-direction at 50 m above the sea floor. The current used in this survey is approximately five times smaller than that available current for commercial surveys [19]. The HED dipole antenna is towed by a vessel in the marine CSEM environment with sea floor receivers to record the electric and magnetic field response. The antenna, which is 100 m in length, is towed at 50 m above the sea floor to avoid bathymetry changes and collision with the stationary sea floor receivers. The antenna is excited with an electric current by a variable frequency ranging between 0.01 Hz - 10 Hz [20]. First, the CSEM trial was done in 1987 and 1988 by Cambridge in collaboration with Scripps on the East Pacific Rise. Their system was based on Scripps' system where they used a neutrally buoyant antenna towed in a deep water environment at 100 m above the sea floor [21]. The antenna was towed at 30 - 40 m above the sea floor with a current of 1000 - 1200 A of a square waveform [22]. A 3D model for shallow water deep targets was reported by [23]. This proposed model was simulated for 750 - 2950 m target depths using the FDTD program in shallow water. The antenna was placed at 30 m above the sea floor with a 0.25 Hz frequency in this 3D proposed model. With this model, he was able to improve the delineation from a 1.05 km to 1.95 km target depth [23]. This work premise deals with the comparison study of the new and conventional antennas' electromagnetic signal strength. The antenna was positioned in a deep water environment to know the exact position where the antenna can give better delineation of the hydrocarbon reservoir. The antenna orientation study was also done for antenna stability due to the surface waves in the CSEM environment.

2. Preliminary Knowledge about Maxwell's Equations and Its Significance in SBL

Maxwell's equations explain the physics of the Controlled Source Electromagnetic Method (CSEM) having four vector functions: electric field, magnetic induction, dielectric displacement and magnetic field H as given below [24].

$$\nabla \cdot \mathbf{D} = \rho \quad (1)$$

$$\mathbf{D} \cdot \mathbf{B} = 0 \quad (2)$$

$$\nabla \times \mathbf{E} = -\frac{\partial \mathbf{B}}{\partial t} \quad (3)$$

$$\nabla \times \mathbf{H} = \mathbf{J} + \frac{\partial \mathbf{D}}{\partial t} \quad (4)$$

The charge density is denoted by ρ (C/m^3), current density (A/m^2), time $t(s)$ and ∇ is the operator as given

in the operator as given in Equations (1)-(4). Equation (1) is Gauss's law, which states that the flux of a given charge through any enclosed surface remains the same. Equation (2) shows the magnetic field divergence, which is stated as the magnetic field divergence is zero. Equation (3) is about Faraday's law: electric fields induced due to a change of a magnetic field will be produced by a current enclosed by an amperian loop, and the moving charges will induce a magnetic field. The constitutive relation between the field quantities in a macroscopic media is very complicated for homogenous regions. The constitutive relation can be written as:

$$\mathbf{D} = \epsilon \mathbf{E} \quad (5)$$

$$\mathbf{B} = \mu \mathbf{H} \quad (6)$$

$$\mathbf{J} = \sigma \mathbf{E} \quad (7)$$

To simplify the electromagnetic problems, Equation 6 becomes:

$$\mathbf{B} = \mu_0 \mathbf{H} \quad (8)$$

In the CSEM, the survey transmitter has an additional source term J_s so the Equation (7) becomes:

$$\mathbf{J} = \sigma \mathbf{E} + \mathbf{J}_s \quad (9)$$

Maxwell's Equation (1) and (4) has displacement terms that can be replaced by the constitutive relation Equation (5) to yield:

$$\nabla \cdot \mathbf{E} = \frac{q}{\epsilon} \quad (10)$$

$$\nabla \times \mathbf{H} = \epsilon \frac{\partial \mathbf{E}}{\partial t} + \mathbf{J} \quad (11)$$

A low frequency is used in the marine controlled electromagnetic survey so that quasi stationary approximations can be used for Maxwell's equations which eliminates the displacement terms. Maxwell's equation is approximated by the diffusion equation rather than the wave equation by the removal of the displacement terms. For electric or magnetic fields, harmonic time variations $e^{-i\omega t}$ are assumed where (ω) is the angular frequency and i is the complex number, then by putting Equation (8) into Equation (3) and including the source term J_s , then Equations (3) and (11) will become:

$$\nabla \times \mathbf{E} = i\mu_0 \omega \mathbf{H} \quad (12)$$

$$\nabla \times \mathbf{H} - \sigma \mathbf{E} = \mathbf{J}_s \quad (13)$$

$$\nabla \times \mathbf{H} = \epsilon \frac{\partial \mathbf{E}}{\partial t} + \sigma \mathbf{E} + \mathbf{J} \quad (14)$$

$$\nabla \times \mathbf{E} = -\mu \frac{\partial \mathbf{H}}{\partial t} \quad (15)$$

$$\nabla^2 \mathbf{H} - \sigma \mu \frac{\partial \mathbf{H}}{\partial t} - \epsilon \mu \frac{\partial^2 \mathbf{H}}{\partial t^2} = 0 \quad (16)$$

$$\nabla^2 \mathbf{E} - \sigma \mu \frac{\partial \mathbf{E}}{\partial t} - \epsilon \mu \frac{\partial^2 \mathbf{E}}{\partial t^2} = 0 \quad (17)$$

$$E_x = E_0 \exp(j\omega t - \gamma y) \quad (18)$$

$$H_z = H_0 \exp(j\omega t - \gamma y) \quad (19)$$

$$\gamma = j\omega \sqrt{\epsilon \mu - j \sigma \mu / \omega} = \alpha + j\beta \quad (20)$$

where γ is the propagation constant, ϵ permittivity, μ permeability, σ conductivity, α attenuation factor, β phase factor and $\omega = 2\pi f$ the angular frequency as given in equation (20). Electromagnetic wave propagation can be described by a wave number k as given in Equation (21) [25].

$$k = \omega \sqrt{\mu \epsilon + i \sigma \mu / \omega} = \frac{\omega}{c_p} + i/\delta \quad (21)$$

where k is the wave number and $i = \sqrt{-1}$ is the complex number, C_p is the phase velocity and δ is the skin depth. The first term in Equation (21), inside the square root represents the displacement current and the second term represents the conduction current in Maxwell's equation.

3. Methodology

CST (Computer simulation technology) software based

on the Finite Integration Method (FIM) is used to simulate the proposed survey area of the seabed model. Computer Simulation Technology (CST) is used to discretize each of Maxwell's equations at a low frequency to investigate the resistivity contrast. For the finite integration technique, computer simulation technology software is used as a tool for low frequencies to solve any problem. FIM was used to detect deep target hydrocarbon below 3000 m from the sea floor by using CST software. CST software was used to detect deep target hydrocarbon at 4000 m underneath the seabed. The model area was assigned as 40×40 km to replicate the real seabed environment with various target positions. There were a few steps involved in generating the CST simulated model. The first step was to set parameters for the aluminium antenna. In this case, a 270 m length, frequency of 0.125 Hz and current of 1250 A is used to excite the antenna. The second step was to set parameters for the model. The air thickness was set as 500 m, sea water depth of 1000 m, overburden thickness of 1000 m, hydrocarbon thickness of 100 m and under burden thickness of 1000 m with their different conductivities and permeability values (**Table 1**). The antenna position was changed from 970 m until reaching 30 m with 40 m intervals each from the sea floor in sea water. The third step was to apply electric boundary conditions (**Table 2**). The fourth step was to run a low frequency full wave solver to simulate the sea bed model.

Table 1. Relative permittivity, conductivity values of air, sea water, overburden/under burden and hydrocarbon.

| Material parameters | Air | Sea water | Under burden/Overburden | Hydrocarbon |
|-----------------------------|--------------|-----------|-------------------------|-------------|
| Relative permittivity | 1.006 | 81 | 30 | 4 |
| Conductivity (S/m) | $1.0E^{-11}$ | 4 | 1.500 | 0.001 |
| Thermal conductivity (W/k) | 0.024 | 0.593 | 2 | 0.492 |
| Density(kg/m ³) | 1.293 | 1025 | 2600 | 900 |

Table 2. Simulated model parameters with different resistive layers (air, sea water, overburden and under burden).

| Antenna position (m) | Air thickness (m) | Under burden/over burden (m) | Hydro-carbon thickness (m) | Sea water depth | Frequency (Hz) |
|----------------------|-------------------|------------------------------|----------------------------|-----------------|----------------|
| 270 | 500 | 1000 | 100 | 1000 | 0.125 |
| 240 | 500 | 1000 | 100 | 1000 | 0.125 |
| 210 | 500 | 1000 | 100 | 1000 | 0.125 |
| 180 | 500 | 1000 | 100 | 1000 | 0.125 |
| 150 | 500 | 1000 | 100 | 1000 | 0.125 |
| 120 | 500 | 1000 | 100 | 1000 | 0.125 |
| 90 | 500 | 1000 | 100 | 1000 | 0.125 |
| 60 | 500 | 1000 | 100 | 1000 | 0.125 |
| 30 | 500 | 1000 | 100 | 1000 | 0.125 |

The final step was post processing to generate the simulated data for result analysis at different antenna orientations. Maxwell’s equations for magnetic and electric fields are used as a code in the software to get electric and magnetic field responses with and without HC. The schematic diagram of the proposed seabed model with the CST simulated model is shown in **Figure 1**.

4. Results and Discussion

4.1. New Antenna and Straight Antenna Electromagnetic Field Strength Comparison

The straight and the new dipole antennas’ electric (E) and magnetic (H) field comparison was done to see the electromagnetic signal strength. The new antenna is also a half wavelength antenna. A half wave length antenna was selected due to its superior radiation pattern compared to other wavelengths ($\lambda/4$, $\lambda/8$ and $\lambda/3$). If the antenna length is adjusted without selecting the proper transmitting frequency, then the desirable antenna radiation pattern cannot be achieved; the efficiency and gain of the antenna are decreased as well [26]. This section focuses on the comparison of the new curved antenna electromagnetic field strength to a straight antenna. Comparison of E, B and H field strengths for the straight and new antennas is given in **Table 3**. This new antenna design aims to be used for deep target hydrocarbon exploration. The conventional antenna (straight antenna) signal strength in deep target areas is very low so the presence of hydrocarbon reservoirs cannot be predicted. This new antenna design shows an 804% increase in electric (E) field strength and a 278% increase in magnetic (H) field strength over the straight dipole antenna. This increase in the electric flux density is due to the large number of electric field lines passing through the unit area due to the focusing of the electromagnetic

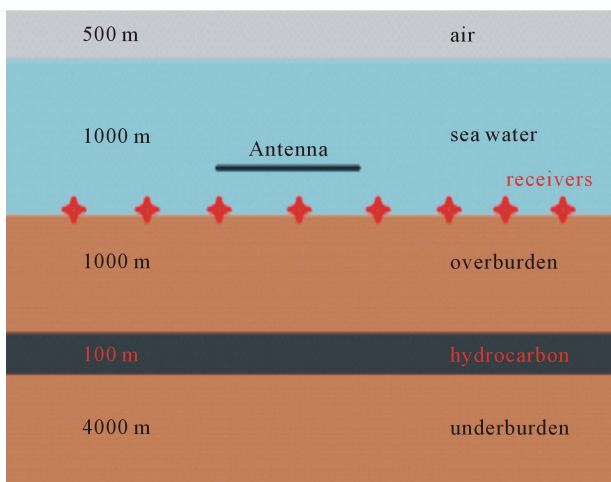


Figure 1. Schematic diagram of the proposed sea bed model.

Table 3. E, B and H field comparison of straight and new dipole antennas.

| Antenna Type | E field (V/m) | B field (Vs/m ²) | H field (A/m) |
|-----------------|-----------------------|------------------------------|-----------------------|
| Straight | $4.13 \times E^{-03}$ | $6.01 \times E^{-11}$ | $4.78 \times E^{-05}$ |
| New | $3.32 \times E^{-02}$ | $1.29 \times E^{-10}$ | $1.03 \times E^{-04}$ |
| Straight dipole | $4.31 \times E^{-03}$ | $5.76 \times E^{-10}$ | $4.58 \times E^{-04}$ |
| New dipole | $3.74 \times E^{-02}$ | $2.18 \times E^{-09}$ | $1.73 \times E^{-03}$ |

waves which increases the electric flux density of the new antenna [27]. This increment of signal strength makes it favorable for deep-target hydrocarbon reservoir detection.

4.2. Antenna Position Study for Seabed Logging

The antenna position is very important for better delineation of hydrocarbon reservoirs in marine CSEM environments. The antenna position was changed from the surface of the sea water (970 m - 30 m) from the sea floor for better delineation of hydrocarbon reservoirs.

The antenna position was changed from 970 m until 30 m from the seabed. The comparison of the E_x field between with and without a hydrocarbon reservoir was done as given in **Figure 2**. With a 970 m until 200 m antenna height from the sea floor the percentage difference between with and without hydrocarbon is less than 10%, which means that it cannot be drilled due to a high drilling risk factor. Below 200 m until 30 m it was observed that the E_x field shows a 10.53%, 12.40%, 14.12%, 14.68%, 37.89%, and 53.10%, difference between with and without hydrocarbon reservoirs at 170 m, 130 m, 90 m, 50 m, 40 m and 30 m, respectively. Comparison of the H_z field strength is shown in **Figure 3**. The H_z field strength is higher than the E_x field strength due to the lower magnetic field loss than with the electric field. The H_z field with and without hydrocarbon reservoirs shows an 83.13% difference where as E_x has 53.10% at a 30 m antenna height from the sea floor as shown in **Figure 4**. For better delineation of hydrocarbon reservoirs, it was analyzed that the antenna should be placed at a 30 m height from the sea floor for deep water environments.

4.3. Antenna Orientation Study for Seabed Logging

The orientation of an antenna study was done for the proposed seabed model. This model consisted of five layers with an array of receivers placed on the sea floor. The new antenna orientation in x and y directions was studied in this proposed model in terms of stability and operational cost. The changing of an antenna’s orientation from the y to x direction can be used to reduce the operational cost. Different components of E and H fields

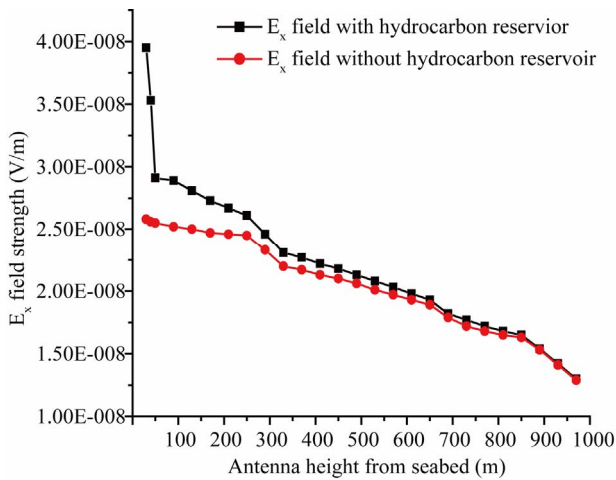


Figure 2. E_x field comparison between with and without a hydrocarbon reservoir of an antenna with a change of position.

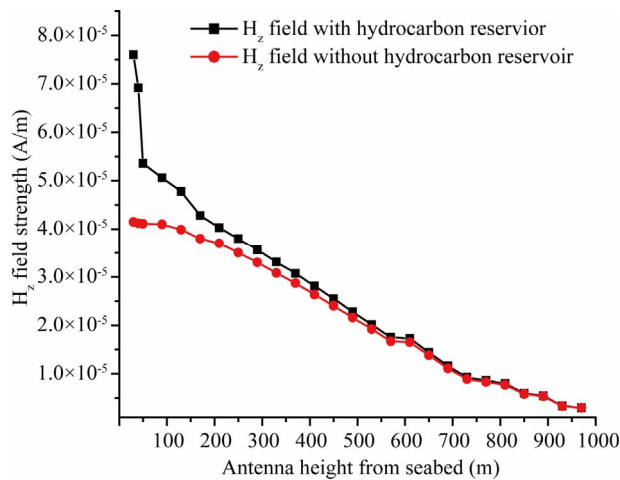


Figure 3. H_z field comparison between with and without hydrocarbon reservoirs of an antenna with the change of position.

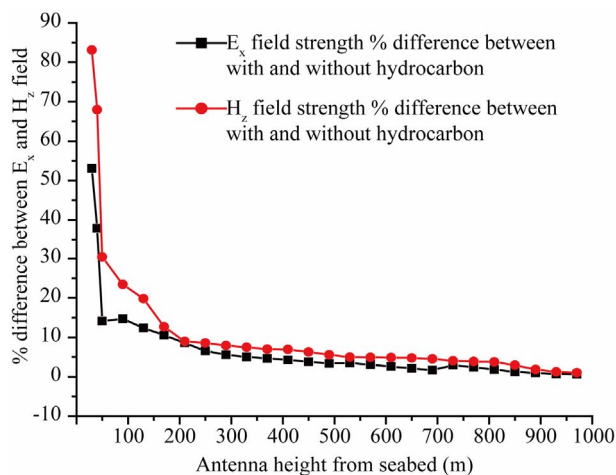


Figure 4. Percentage difference between E_x and H_z field strength at different antenna positions in sea water.

were studied for both x and y oriented antennas for a 4 km target depth. The deep-water model consisting of five layers (air, sea water, overburden, hydrocarbon, and under burden) was created with an array of sea floor receivers placed on the sea floor. The aim of this study was to test the new antenna in the x and y orientation in regards to the operational cost. The antenna was excited with a 1250A current operating at the 0.125 Hz frequency at 30 m above the sea floor. The electric and magnetic field data response was measured with the antenna orientation in the y direction. All electric and magnetic field component responses were plotted and are given (Figures 5-22) to know which components gave better delineation of a hydrocarbon reservoir. For the vertical antenna orientation, a linearly polarized plane wave was travelling in the y direction, then the E_x and H_z components gave information about the hydrocarbon reservoir [25]. From the results, it was also observed that, E_x and H_z gave better delineation of the hydrocarbon reservoir. H_z gave a 21% field strength and electric field of 18% at the km target depth where as other components have not shown any difference.

An electric and magnetic field component study was done in a survey area of (40 km × 40 km) with and without the presence of a hydrocarbon reservoir. E and H field component responses with the new antenna at the 4 km target depth are given (Figures 5-16). The antenna was placed at 30 m above the sea floor in the x direction. The propagation of electromagnetic waves can be predicted by using Maxwell’s equations. An electromagnetic wave traveling in the x direction can be described in terms of the electric field strength E_y and the magnetic field strength H_z . According to Maxwell’s equations, if the direction of the propagation of the electromagnetic waves is in the y direction, then E_x and H_z components gave better hydrocarbon responses as was reported by [25]. From the results, it was analyzed that the E_y and H_z components gave better delineation of the hydrocarbon reservoirs than other components, which is in agreement with Maxwell’s equations. It was observed that E_y and H_z field components gave 12% and 16% responses from the 4km target depth. Changing of the antenna orientation from the y direction to the x direction caused an electric field response decrease from 18% to 12% and the H_z field strength from 21% to 16% but the hydrocarbon reservoir could still be detected at the 4 km target depth. Straight and new antennas with different curvatures were studied with the 4 km target depth to know which antenna gave better delineation of the hydrocarbon reservoirs while the antennas were oriented in the x direction.

The magnetic field response from the 4 km target depth with the new antenna at different T_x and T_y orientation is given (Figures 17-22). There was a significant change in the results when the antenna orientation changes from the

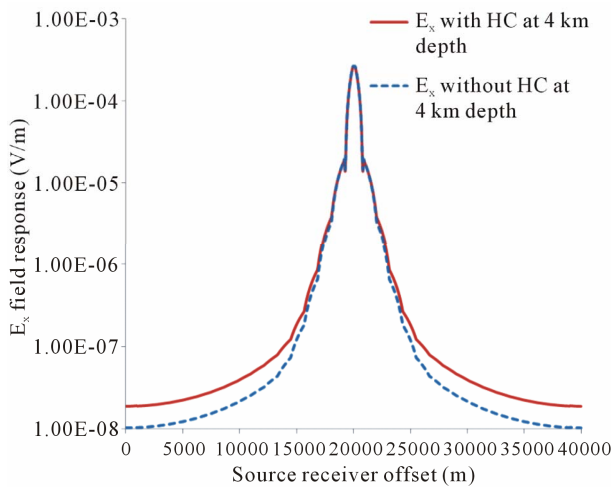


Figure 5. New antennas E_x field responses at 4 km target depth (T_y orientation).

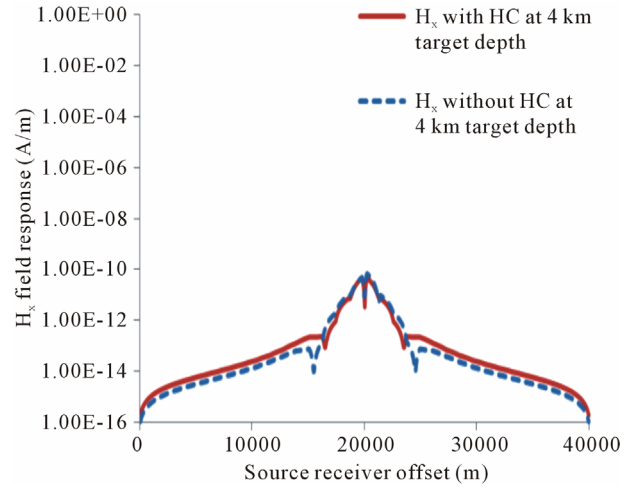


Figure 8. New antenna E_z field responses at 4 km target depth (T_y orientation).

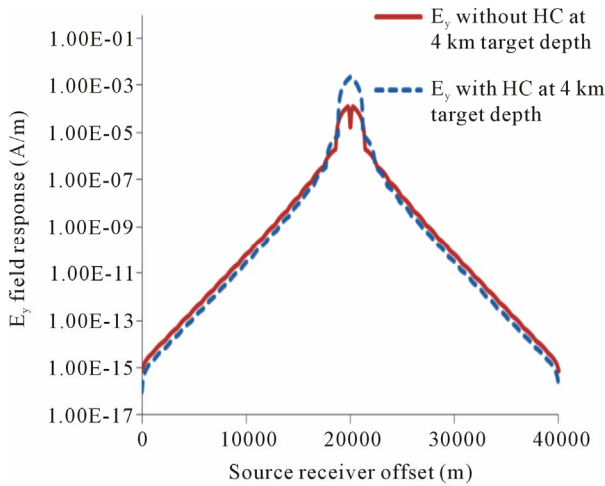


Figure 6. New antenna E_y field responses at 4 km target depth (T_y orientation).

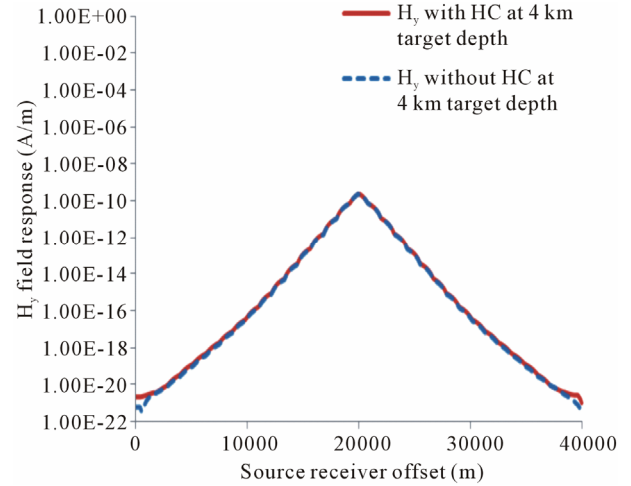


Figure 9. New antenna H_y field responses at 4 km target depth (T_y orientation).

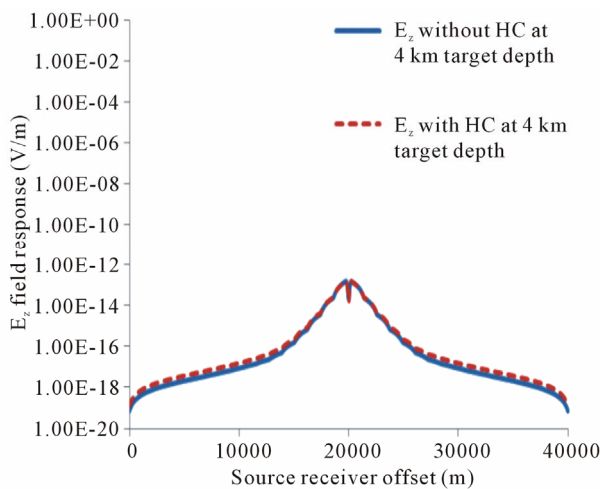


Figure 7. New antenna E_z field responses at 4 km target depth (T_y orientation).

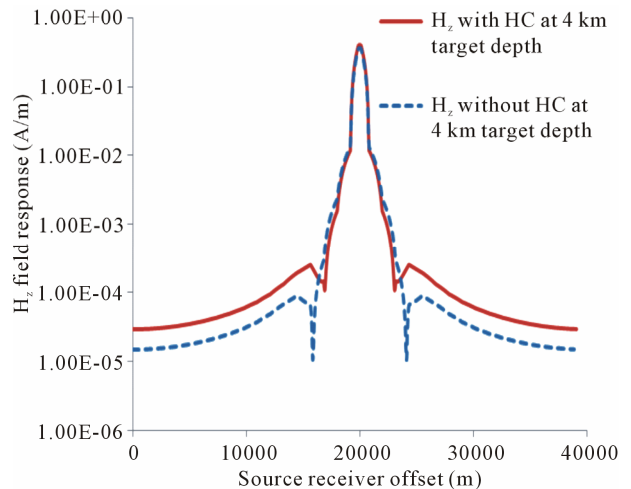


Figure 10. New antenna H_z field responses at 4 km target depth (T_y orientation).

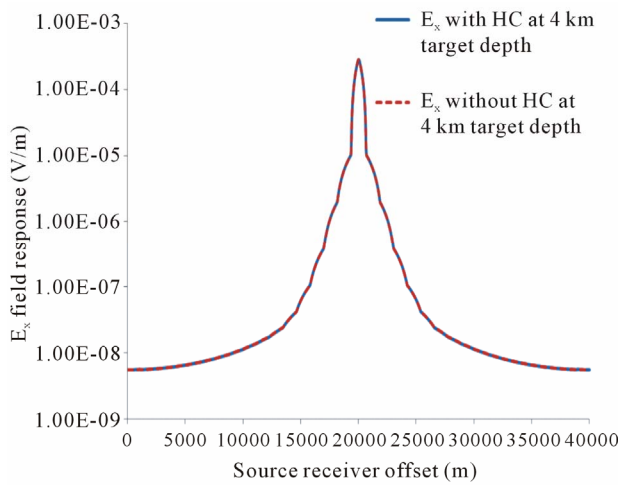


Figure 11. New antenna E_x field responses at 4 km target depth (T_x orientation).

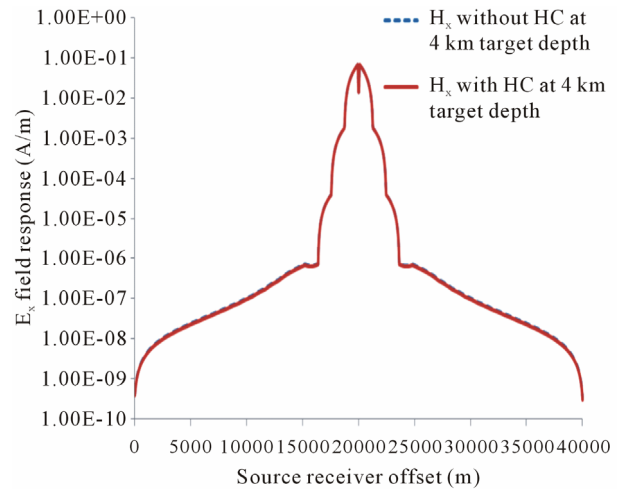


Figure 14. New antenna H_x field responses at 4 km target depth (T_x orientation).

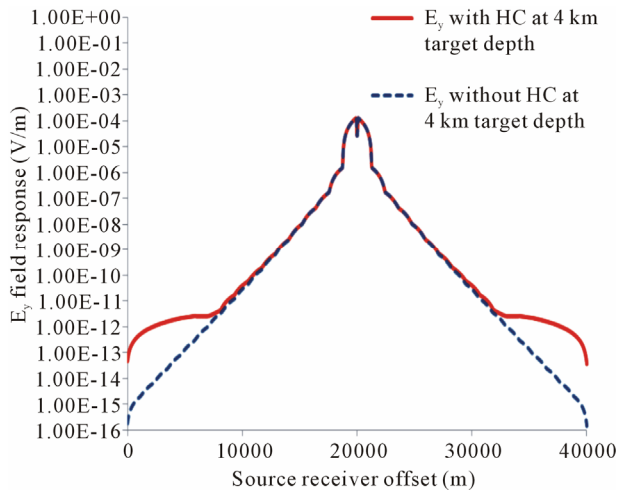


Figure 12. New antenna E_y field response at 4 km target depth (T_x orientation).

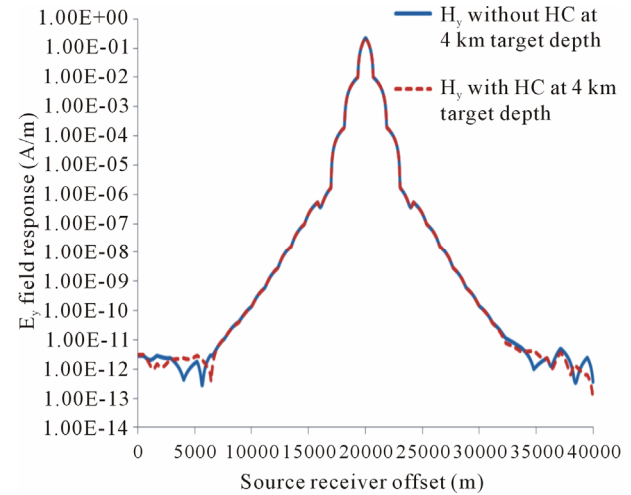


Figure 15. New antenna H_y field responses at 4 km target depth (T_x orientation).

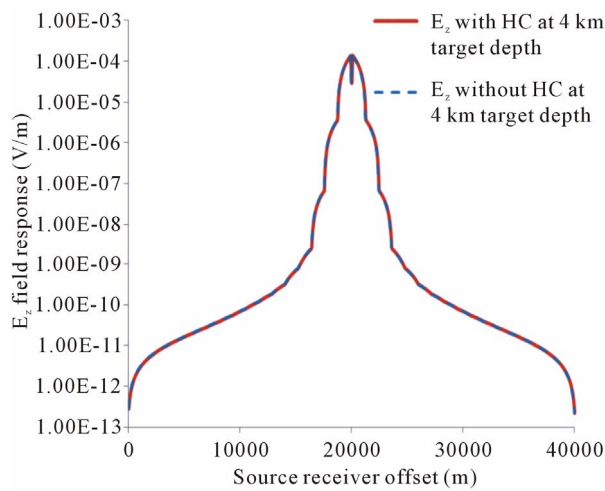


Figure 13. New antenna E_z field responses at 4 km target depth (T_x orientation).

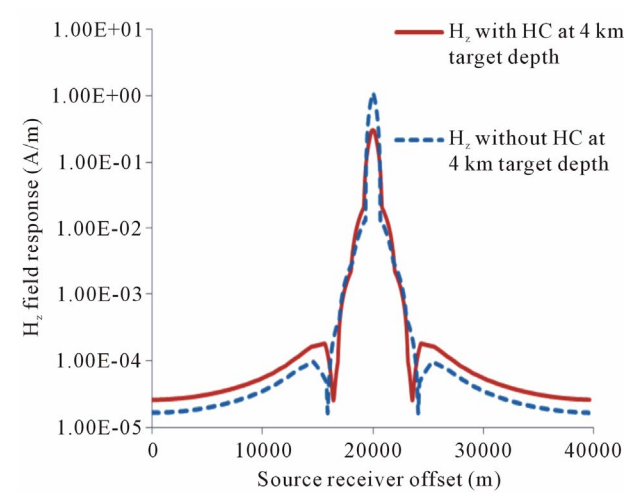


Figure 16. New antenna H_z field responses at 4 km target depth (T_x orientation).

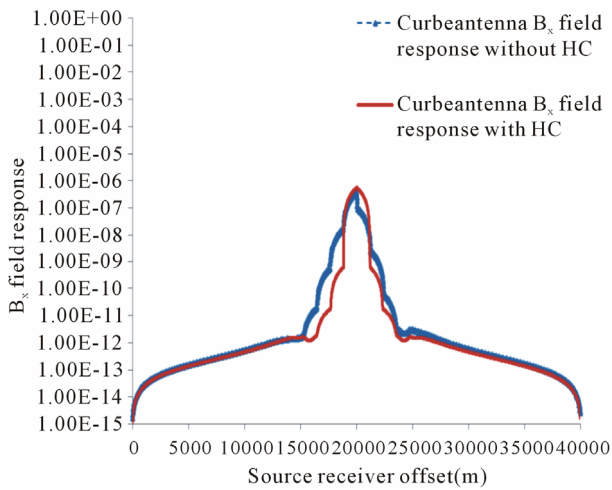


Figure 17. New antenna B_x field responses at 4 km target depth (T_y orientation).

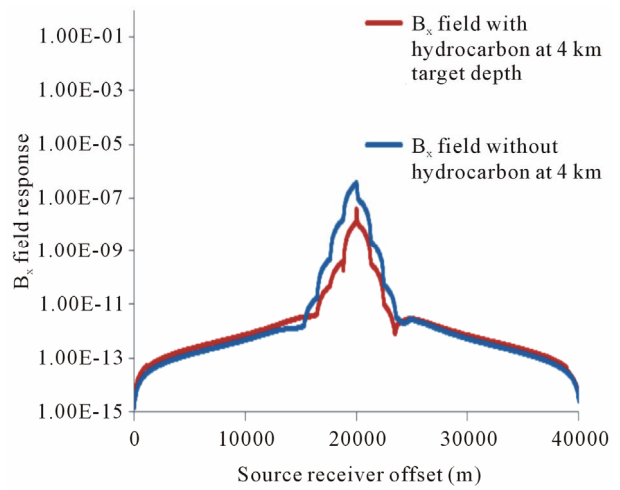


Figure 20. New antenna B_x field responses at 4 km target depth (T_x orientation).

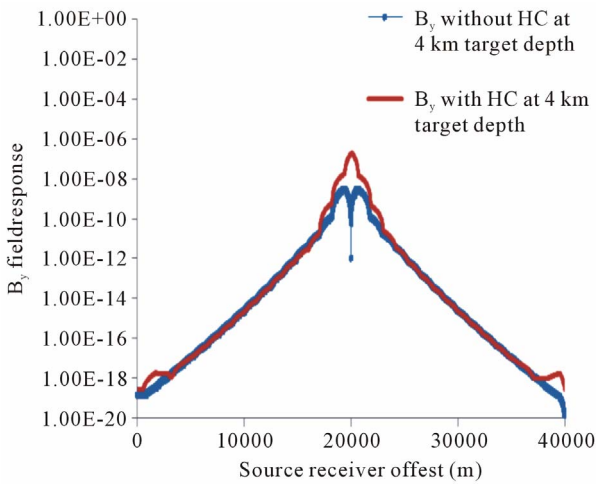


Figure 18. New antenna B_y field responses at 4 km target depth (T_y orientation).

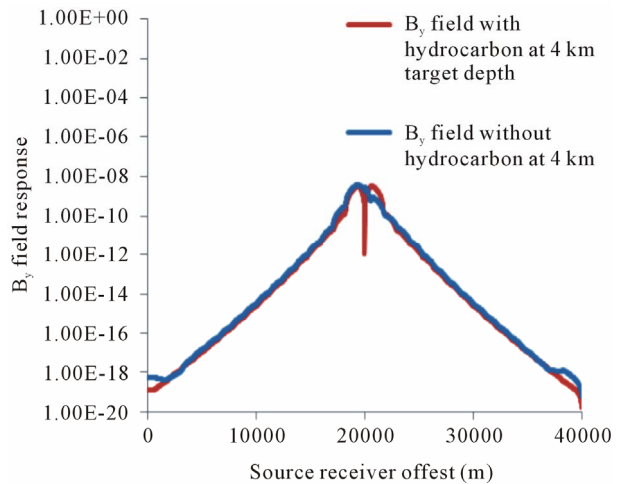


Figure 21. New antenna B_y field responses at 4 km target depth (T_x orientation).

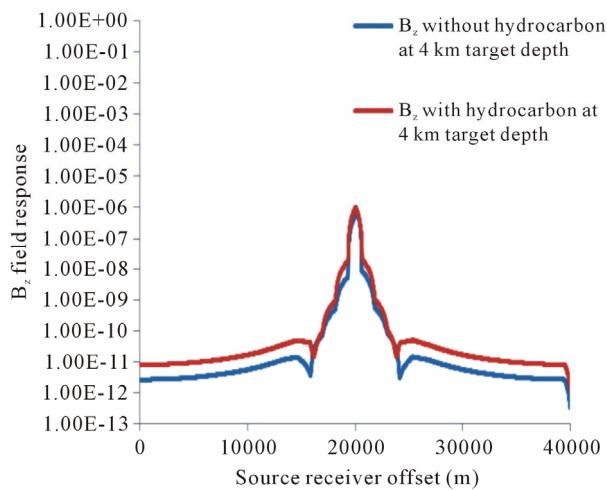


Figure 19. New antenna B_z field responses at 4 km target depth (T_y orientation).

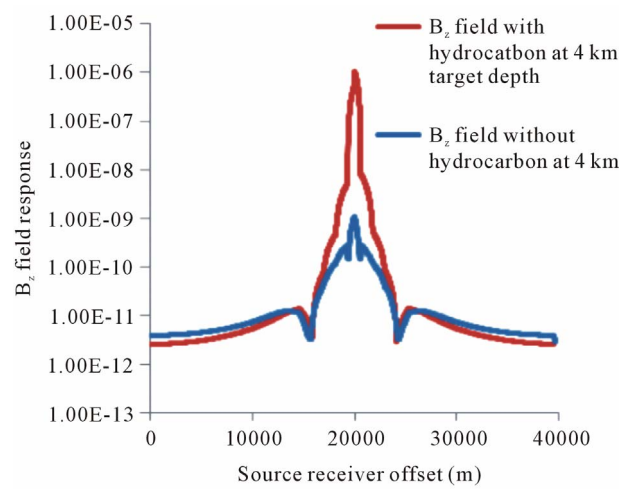


Figure 22. New antenna B_z field responses at 4 km target depth (T_x orientation).

Table 4. Antenna orientation study with E, B and H fields components.

| Antenna orientation | Frequency (Hz) | T _x and T _y location (m) | % Difference with and without HC (E _x) | % Difference with and without HC (E _y) | % Difference with and without HC (E _z) |
|---------------------|----------------|--|--|--|--|
| T _x | 0.125 | 30 | 1 | 12 | 1.3 |
| T _y | 0.125 | 30 | 18 | 0.5 | 0.8 |
| | | | (B _x) % difference | (B _y) % difference | (B _z) % difference |
| T _x | 0.125 | 30 | 0.5 | 0.9 | 5 |
| T _y | 0.125 | 30 | 0.8 | 1.3 | 10 |
| | | | (H _x) % difference | (H _y) % difference | (H _z) % difference |
| T _x | 0.125 | 30 | 1 | 0.6 | 16 |
| T _y | 0.125 | 30 | 1.5 | 0.7 | 21 |

y direction to the x direction. For T_y antenna orientation, the B_z component of the magnetic field shows a 10% delineation between with and without hydrocarbon reservoirs where as for T_x, there is a 5% difference between with and without hydrocarbon reservoirs. For antenna x, the orientation magnetic field B_z component as not able to detect the hydrocarbon reservoir at the 4 km target depth.

The new antenna gave better delineation of hydrocarbon reservoirs than other curvatures and the straight antenna. From the results, it was analyzed that the electric field E_x and magnetic field H_z responses decreased from 18% to 12% and 21% to 16%, respectively. The comparison of the antenna orientation with its field components is given in **Table 4**. The antenna orientation study was done due to the surface wave in shallow water, which can disturb its stability. This instability of the antenna may affect the data collected by the CSEM survey. To make the antenna stable, it needs to be a two tail fish and tow fish for antenna stability, which will increase the operational cost. The new antenna in the x direction can also detect the 4 km target depth and have more stability than the antenna in the y direction. This section concludes that in terms of antenna stability and operational cost, the new antenna with a T_x orientation can still detect the hydrocarbon reservoir at the 4 km target depth although the field strength decreases by changing the antenna orientation. The new antenna with the x orientation can also be used for the 4 km target depth to reduce the operational cost and to predict the presence of the deep target hydrocarbon reservoir accurately.

5. Conclusion

A straight antenna used for seabed logging was compared with the new antenna. The new antenna shows an increase of 804% electric and 278% magnetic field strength over the antenna currently used for seabed logging. The antenna at the 30 m height in a deep water environment gave an 83.13% difference with and without

the hydrocarbon reservoir. From the antenna orientation results, it was analyzed that changing the orientation of an antenna from the y direction to the x direction caused the electric (E_x) field response to decrease from 18% to 12% and the (H_z) field strength from 21% to 16% but the hydrocarbon reservoir could still be detected at the 4 km target depth.

REFERENCES

- [1] L. MacGregor and M. Sinha, "Use of Marine Controlled-Source Electromagnetic Sounding for Sub-Basalt Exploration," *Geophysical Prospecting*, Vol. 48, No. 6, 2000, pp. 1091-1106. [doi:10.1046/j.1365-2478.2000.00227.x](https://doi.org/10.1046/j.1365-2478.2000.00227.x)
- [2] B. Tossman, D. Thayer and W. Swartz, "An Underwater Towed Electromagnetic Source for Geophysical Exploration," *IEEE Journal of Oceanic Engineering*, Vol. 4, No. 3, 1979, pp. 84-89. [doi:10.1109/JOE.1979.1145427](https://doi.org/10.1109/JOE.1979.1145427)
- [3] S. Johansen, *et al.*, "Subsurface Hydrocarbons Detected by Electromagnetic Sounding," *First Break*, Vol. 23, No. 3, 2005, pp. 31-36.
- [4] N. Yahya, M. N. Akhtar, N. Nasir, A. Shafie, M. S. Jabeli and K. Koziol, "CNT Fibres/Aluminium-NiZnFe₂O₄ Based EM Transmitter for Improved Magnitude vs Offset (MVO) in a Scaled Marine Environment," *Journal of Nanoscience and Nanotechnology*, 2011, in press.
- [5] N. Yahya, M. N. Akhtar, N. Nasir, H. Daud and M. Narahari, "Forward Modeling of Seabed Logging by Finite Integration (FI) and Finite Element (FE) Methods," *Digital Subscriber Line*, 2011, in press.
- [6] N. Yahya, M. Kashif, H. Daud, H. M. Zaid, A. Shafie, N. Nasir and A. See, "Fabrication and Characterization of Y₃O-XLaXFe₃O₁₂-PVA Composite as EM Waves Detector," *International Journal of Basic & Applied Sciences*, Vol. 9, No. 9, 2009, pp. 131-134.
- [7] N. Nasir, N. Yahya, M. N. Akhtar, M. Kashif, A. Shafie, H. Daud and H. M. Zaid, "Magnitude Verses Offset Study with EM Transmitter in Different Resistive Medium," *Journal of Applied Sciences*, Vol. 11, No. 7, 2011, pp. 1309-1314. [doi:10.3923/jas.2011.1309.1314](https://doi.org/10.3923/jas.2011.1309.1314)
- [8] M. N. Akhtar, N. Yahya, H. Daud, A. Shafie, H. M. Zaid,

- M. Kashif and N. Nasir, "Development of EM Wave Guide Amplifier Potentially Used for Seabed Logging," *Journal of Applied Sciences*, Vol. 11, No. 7, 2011, pp. 1361-1365. [doi:10.3923/jas.2011.1361.1365](https://doi.org/10.3923/jas.2011.1361.1365)
- [9] M. Unsworth, "New Developments in Conventional Hydrocarbon Exploration with Electromagnetic Methods," *CSEG Recorder*, Vol. 30, No. 4, 2005, pp. 34-38.
- [10] P. Clemmow, "The Theory of Electromagnetic Waves in a Simple Vanisotropic Medium," *Proceedings of the Institution of Electrical Engineers*, Vol. 110, No. 1, 1963, pp. 101-106. [doi:10.1049/piee.1963.0015](https://doi.org/10.1049/piee.1963.0015)
- [11] F. N. Kong, H. Weterdahl, S. Ellingsrud, T. Eidesmo and S. Johansen, "A Possible Direct Hydrocarbon Indicator for Deep Sea Prospects Using EM Energy," *Oil and Gas Journal*, Vol. 100, No. 19, 2002, pp. 30-38.
- [12] M. N. Akhtar, N. Yahya, K. Koziol and N. Nasir, "Synthesis and Characterizations of $\text{Ni}_{0.8}\text{Zn}_{0.2}\text{Fe}_2\text{O}_4$ —MWCNTs Composites for Their Application in Sea Bed Logging," *Ceramics International*, Vol. 37, No. 8, 2011, pp. 3237-3245. [doi:10.1016/j.ceramint.2011.05.113](https://doi.org/10.1016/j.ceramint.2011.05.113)
- [13] M. C. Sinha, P. D. Patel, M. J. Unsworth, T. R. E. Owen and M. G. R. MacCormack, "An Active Source Electromagnetic Sounding System for Marine Use," *Marine Geophysical Research*, Vol. 12, No. 1-2, 1990, pp. 59-68.
- [14] J. Nordskog and L. Amundsen, "Asymptotic Airwave Modeling for Marine Controlled-Source Electromagnetic Surveying," *Geophysics*, Vol. 72, No. 6, 2007, pp. F249-F255. [doi:10.1190/1.2786025](https://doi.org/10.1190/1.2786025)
- [15] Y. Li and K. Key, "2D Marine Controlled Electromagnetic Modeling: An Adaptive Finite Element Algorithm," *Geophysics*, Vol. 72, No. 2, 2007, pp. 51-62. [doi:10.1190/1.2432262](https://doi.org/10.1190/1.2432262)
- [16] F. N. Kong, S. E. Johnstad and T. Roesten, "Characteristics of Scattered Fields from Hydrocarbon Layers in Seabed Logging," *PIERS Online*, Vol. 2, No. 6, 2006, pp. 585-588. [doi:10.2529/PIERS060821070831](https://doi.org/10.2529/PIERS060821070831)
- [17] P. D. Young and C. S. Cox, "Electromagnetic Active Source Sounding Near the East Pacific Rise," *Geophysical Research Letters*, Vol. 8, No. 10, 1981, pp. 1043-1046. [doi:10.1029/GL008i010p01043](https://doi.org/10.1029/GL008i010p01043)
- [18] E. Um and D. Alumbaugh, "On the Physics of the Marine Controlled-Source Electromagnetic Method," *Geophysics*, Vol. 72, No. 2, 2007, pp. WA13-WA26. [doi:10.1190/1.2432482](https://doi.org/10.1190/1.2432482)
- [19] S. Ellingsrud, T. Eidesmo, S. Johansen, M. C. Sinha, L. M. MacGregor and S. Constabl, "The Leading Edge," *Society of Economic Geologists*, Vol. 21, No. 10, 2002, pp. 972-982. [doi:10.1190/1.1518433](https://doi.org/10.1190/1.1518433)
- [20] S. C. Constable, C. S. Cox and A. D. Chave, "Offshore Electromagnetic Surveying Techniques," 1986 SEG Annual Meeting, 1986.
- [21] P. D. Aversana and M. Vivier, "Geophysical Prospecting, Expanding the Frequency Spectrum in Marine CSEM Applications," *Geophysical Prospecting*, Vol. 57, No. 4, 2008, pp. 573-590.
- [22] F. Maa and F. A. Roth, "Improving Seabed Logging Sensitivity in Shallow Water through Up-Down Separation," EGM 2007 International Workshop, Trondheim, 2007.
- [23] J. A. Kong, "Electromagnetic Wave Theory," John Wiley and Sons, New York, 1986.
- [24] A. Shaw, A. I. Al-Shamma'a, S. R. Wylie and D. Toal, "Experimental Investigations of Electromagnetic Wave Propagation in Seawater," *Proceedings of the 36th European Microwave Conference*, Manchester, 10-15 September 2006, pp. 572-575.
- [25] Sodal, "Transmitting Antenna," US Patent No. 0202697, 2006.
- [26] H. Daud, N. Yahya and R. Harun, "Wireless Control Mechanism for EM Source and Receiver Positioning for Offshore Applications," *Journal of Applied Science*, Vol. 11, No. 7, 2011, pp. 1812-5654.